THE JOURNAL OF PHYSICAL CHEMISTRY B

Article

pubs.acs.org/JPCB

Driving of a Small Solvated Peptide in the IR and THz Range—A Comparative Study of Energy Flow

Gudrun Niehues,[†] Alexey L. Kaledin,[‡] Joel M. Bowman,[‡] and Martina Havenith*[,†]

[†]Lehrstuhl für Physikalische Chemie II, Ruhr-Universität Bochum, 44780 Bochum, Germany

[‡]Cherry L. Emerson Center for Scientific Computation and Department of Chemistry, Emory University, Atlanta, Georgia 30322, United States

ABSTRACT: We present a comparative study of energy flow from a vibrationally excited solvated dialanine molecule to the surrounding water in the IR and THz range. We employ the driven molecular dynamics (DMD) approach to investigate the energy flow from the solute molecule to water molecules. As a result, we find a more rapid and efficient energy flow from the solute to the water when exciting THz modes compared to IR modes. Our results show a strong coupling of the low frequency mode of the solute and the water dynamics in the THz regime. In contrast, when exciting the IR modes of the solute, we find much more localized motions.

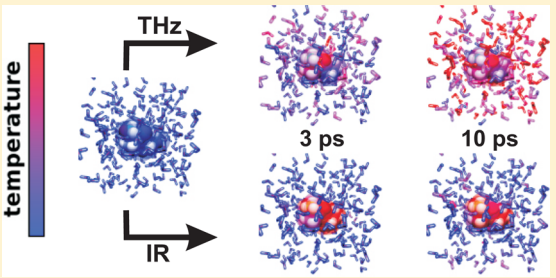

INTRODUCTION

The role of water for biologically relevant processes such as protein folding or enzymatic function is still a matter of debate. The energy flow in peptides as well as proteins has been the focus of several studies: Botan et al.[1] investigated the energy transport through a peptide helix induced by vibrational excitation in a joint experimental and theoretical approach and found a 1D diffusion process along the peptide chain. Leitner[2] investigated the energy flow in proteins to understand the general characteristics of energy flow through residues of proteins. Kim et al.[3] reported the 2D IR spectrum of dialanine in aqueous solution in the amide I′ region and could identify highly localized resonances. Other studies have focused on dynamics of water at specific sites of the solute[4] or specific pathways for energy flow between solute and solvent during isomerizations.[5] Previous studies have investigated the vibrational energy relaxation (VER) process of peptides and proteins using time dependent perturbation theory: For *N*-methylacetamide (NMA), it could be shown that for the amide bands well localized modes could be found, especially at the CO bond. VER of NMA-D in heavy water was found to be dominated in the initial phase by intramolecular vibrational redistribution (IVR) localized near the peptide bond.[6] This process was found to be temperature dependent. In the follow-up study, the sensitivity of the time scale and the mechanism on the solvent surrounding has come into the focus: Zhang, Fujisaki, and Straub have investigated the mode specific VER in NMA/water clusters (involving 0−3 water molecules). They stated an important role for motion associated with water molecules in the mechanism of energy transfer: For NMA-d_1/$(D_2O)_3$/PCM clusters, an evolution of energy flow of the amide I mode into the water was found. Whereas initially the energy flow is dominated by the intramolecular mechanism, later the intermolecular mechanism transferring the energy into the water became dominant.[7] Most investigations focus on IR excitation; in the present paper, we will compare the solute−solvent coupling in the IR frequency range with the THz range.

We present results of a driven MD (DMD)[8−11] study focusing on the energy transfer from the solute to the solvent. We have chosen the DMD method for examining the energy flow because—unlike normal-mode analysis—by strong driving it leads to anharmonic motions and is not bound by the system size. This is of special importance for the description of low frequency modes which have a considerable anharmonicity and describe collective, large amplitude motions. Our results show that in the THz range we find a very efficient coupling of the low frequency modes of the peptide to the water network motions. This coupling facilitates a rapid energy flow from the solute to the solvent. This is shown to differ from the IR, where we find more localized excitations of the intramolecular vibrations. Whereas in the THz range the energy dissipates rapidly into the solvent within the simulation time (10 ps), in the IR only very little dissipation into the water is found.

METHODS

Experimental Section. The experimental setup and the analysis have been described in detail in refs 12 and 13. We have recorded the Fourier transform (FT) spectra of solvated dialanine in two spectral ranges using a Bruker Vertex 80 V FTIR. We have recorded the THz spectra in the range between 50 and 350 cm^{-1} and in the IR in the frequency range between 1100 and 1525 cm^{-1}, using a Bruker liquid cell with CVD-diamond windows (500 ± 100 μm thickness, Diamond Materials, GmbH) as sample holders. To adjust the thickness

Received: March 5, 2012
Revised: July 27, 2012
Published: July 30, 2012

   dx.doi.org/10.1021/jp3021358 | *J. Phys. Chem. B* 2012, 116, 10020−10025

of the liquid layer, polyethylene spacers with a thickness d of 40 ± 1 μm were used. The precise cell thickness was determined by measurements of the etalon fringes in the empty cell. The sample compartment including the liquid cell was kept under nitrogen purged conditions. As a separation between the sample compartment and the evacuated rest of the spectrometer, polyethylene and KBr flaps were used when measuring in the THz and IR range, respectively. For each spectrum, 256 scans were averaged with a 2 cm^{-1} resolution. In order to minimize etalon effects due to the windows, a moving average with a width of 15 cm^{-1} was used. The liquid samples were temperature controlled and kept at 20 ± 0.1 °C.

For the IR measurements, a nitrogen cooled MCT detector and a KBr beamsplitter were used. For the THz measurements, the spectrometer was equipped with a liquid helium cooled Si bolometer (Infrared Laboratories) as a detector and a Mylar Multilayer 6 μm beamsplitter. Water spectra were measured as a reference. We have determined the difference in the absorption coefficient $\Delta\alpha_{sample,water}$ between the aqueous dialanine solutions and water. Here, the difference in absorption of the sample solution to water was calculated according to

$$\Delta\alpha_{sample,water}(\omega) = \frac{1}{d}\ln\left(\frac{I_{water}(\omega)}{I_{sample}(\omega)}\right) \tag{1}$$

In the THz range, the absolute absorption coefficient of water α_{water} was determined by measuring the absorption of the water when varying the thicknesses of the liquid layers, as described in detail in refs 12 and 13. The absolute absorption coefficient of the sample α_{sample} could be determined by adding $\Delta\alpha_{sample,water}$ to the absolute absorption coefficient of water α_{water}:

$$\alpha_{sample} = \alpha_{water} + \Delta\alpha_{sample,water} \tag{2}$$

Driven Molecular Dynamics (DMD). The DMD method has been explained in previous papers in detail.[8−11] Here, we just want to give a short summary. The concept of the DMD method is to apply an external, harmonic driving force at the driven frequency ω_n. This is done by adding a driving term $U(t)$ to the Hamiltonian H_0. Under mild driving conditions, this method can be used to determine normal-mode frequencies. The driving term $U(t)$ was implemented into the velocity Verlet integration of the TINKER program package.[14]

The Hamiltonian of a system consisting of N atoms used in the DMD simulation is described by

$$H(\mathbf{p}, \mathbf{q}, t) = H_0(\mathbf{p}, \mathbf{q}) + U(t) \tag{3}$$

where $\mathbf{p}$ and $\mathbf{q}$ represent the $3N$ atomic Cartesian coordinates and momenta, respectively. The Hamiltonian H_0 is given by

$$H_0(\mathbf{p}, \mathbf{q}) = \sum_i \sum_\alpha \frac{p_{\alpha,i}^2}{2m_i} + V(\mathbf{q})$$
$$i = 1, ..., N, \quad \alpha = x, y, z \tag{4}$$

The driving term $U(t)$ depends on the internuclear distances r_{ij} and is given by

$$U(t) = \sum_i \sum_j \lambda_{ij} r_{ij} \sin(\omega t) \tag{5}$$

where λ_{ij} are the coupling constants and ω is the driving frequency. We obtain the following Hamilton equations of motion

$$\dot{q}_{\alpha,i}(t) = \frac{\partial H}{\partial p_{\alpha,i}} = \frac{p_{\alpha,i}(t)}{m_i} \tag{6}$$

$$\dot{p}_{\alpha,i}(t) = -\frac{\partial H}{\partial q_{\alpha,i}} \tag{7}$$

$$= -\frac{\partial H_0}{\partial q_{\alpha,i}} - \sum_{j\neq i} \lambda_{ij}\frac{\partial r_{ij}}{\partial q_{\alpha,i}} \sin(\omega t) \tag{8}$$

$$= -\frac{\partial V}{\partial q_{\alpha,i}} - \sum_{j\neq i} \lambda_{ij}\frac{q_{\alpha,i} - q_{\alpha,j}}{r_{ij}} \sin(\omega t)$$
$$i = 1, ..., N, \quad \alpha = x, y, z$$

In order to quantify the absorption, we have calculated the average total internal energy of the system after a finite time t of driving, i.e.,

$$\langle E\rangle = \frac{1}{M}\sum_{i=0}^{M} H_0(t_i) \tag{9}$$

where $M = t/\Delta t$ and the potential energy at $t = 0$ is the potential energy zero point. At resonant frequencies, the absorbed energy increases rapidly with increasing time, whereas at nonresonant frequencies it remains small and oscillates in time.

Whereas previous DMD studies concentrated on the investigation of the spectra of isolated molecules, our focus here is a detailed investigation of the interaction of a solute with the embedding medium, water, on a molecular scale. To get deeper insights into the character of this interplay at different frequencies, we studied dialanine in aqueous solution. Dialanine, as an isolated molecule, has been investigated before with the DMD method.[11] Here, we investigate the peptide in solution; consequently, a zwitterionic form of the molecule was employed. We applied the driving term only to the solute molecule and observed the energy dissipation into the solvent. Accordingly, λ_{ij} were chosen to be 10^{-4} Hartree/bohr for i, j on dialanine and λ_{ij} were set to 0 otherwise. This allows us to pursue our goal of investigating the coupling between the solute and the solvent at resonant frequencies.

For the potential energy contributions of the solute, the OPLS-AA[15] force field was used; for water, the flexible TIP3P model[16] was employed. We have used periodic boundary conditions. The size of the system was varied due to the high computational cost: Most of the simulations were performed for a smaller system consisting of a dialanine molecule and 207 water molecules in a cubic box with a length of 18.643 Å. To investigate the energy flow into the surrounding water when driving at a THz frequency, a larger system of a dialanine molecule and 3993 water molecules in a cubic box with a length of 49.323 Å was simulated.

Prior to the driving simulation, an energy minimization using a quasi-Newton nonlinear optimization[17] was performed, until the rms gradient was below 10^{-5} kcal/(mol Å). The initial velocities of the atoms were set to zero. This starting point corresponds to a temperature of $T = 0$ K. At first glance, this appears a very special case. However, by continuously driving the molecule, the constant energy flow into the solvent leads to

dx.doi.org/10.1021/jp3021358 | J. Phys. Chem. B 2012, 116, 10020−10025

an increase in the average velocities and this corresponds to higher temperatures. All simulations were run for 10 ps with 10 000 integration steps.

RESULTS

Experimental Section. In Figure 1, we show the THz spectra of solvated dialanine (for five concentrations) and

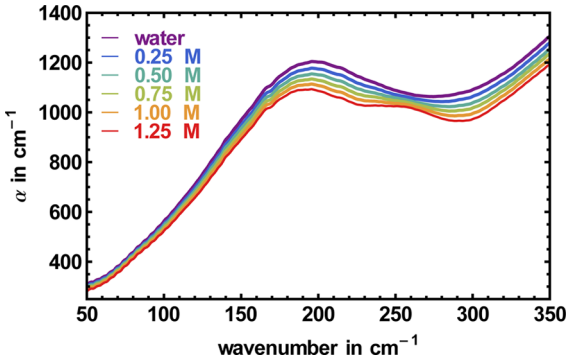

Figure 1. Shown is the measured α_{sample} vs wavenumber in the THz range (50−350 cm^{-1}) when varying the concentrations of dialanine in the solution.

compare this with the spectrum of bulk water. As a general trend, we observe a decrease in absorption with increasing concentration of dialanine between 50 and 350 cm^{-1}. In our previous publications,[18] we could explain this as the THz defect: The decrease is attributed to a decrease of THz absorption due to the exclusion of absorbing water molecules by the presence of the solute. This volume exclusion (based on the partial molar volume of dialanine[19]) corresponds to a partial volume of 3−14% within the investigated concentration range.

If we use this to calculate the partial absorption of water by $\alpha_{part} = \alpha_{solution} - \beta\alpha_{water}$, with β describing the partial volume of water as deduced from the partial volume of dialanine, we obtain the results which are shown in Figure 2A. As a result, we find broad absorption peaks with a maximum around 170 and 250 cm^{-1}. On the basis of the almost linear scaling with the peptide concentration, we attribute this to the absorption of the solute with its hydration shell. Figure 2B shows the molar absorption coefficients (i.e., scaled by the concentration of dialanine) in the investigated THz range. These show a small nonlinearity in the concentration dependence of the absorption coefficients.

For comparison, we show in Figure 3A the IR spectra between 1100 and 1500 cm^{-1} (plotted is the difference to water absorption). In this frequency range, we find distinct peaks, which can be assigned to localized dialanine modes. For the IR, we find a strictly linear scaling of the absorption with increasing dialanine concentration (see Figure 3B, here, the absorption coefficients, are in analogy to Figure 2B scaled by concentration of dialanine).

Thus, we distinguish between characteristic modes of solvated dialanine in the IR and broad absorption bands of the coupled dialanine−water network motions in the THz range. The observed line broadening of the THz modes indicates a pronounced coupling of the solute with the solvent. This will be investigated in more detail in the following section.

Driven Molecular Dynamics. As a first step, a normal-mode analysis (NMA) of the system with one dialanine molecule and 207 water molecules was carried out. The aim of

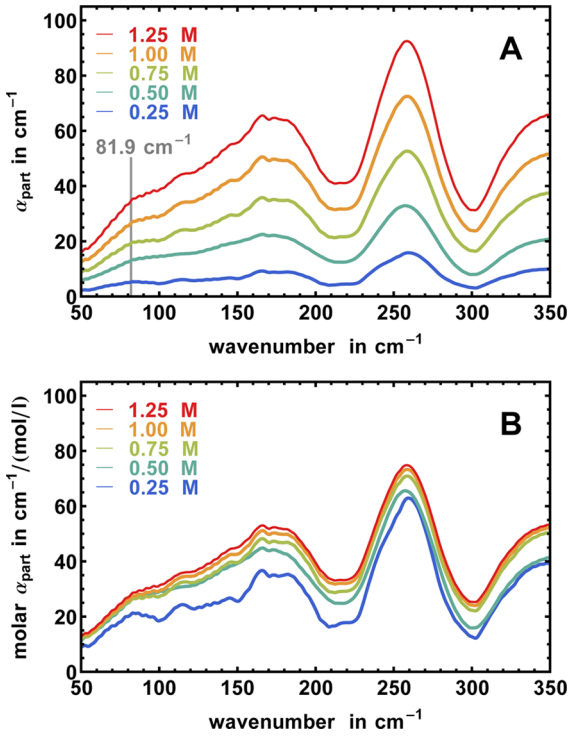

Figure 2. (A) Shown is the partial absorption coefficient α_{part} vs wavenumber in the THz range (50−350 cm^{-1}) for five concentrations of dialanine solutions. (B) Shown is the molar partial absorption coefficient α_{part} vs wavenumber in the THz range (50−350 cm^{-1}) for five concentrations of dialanine solutions.

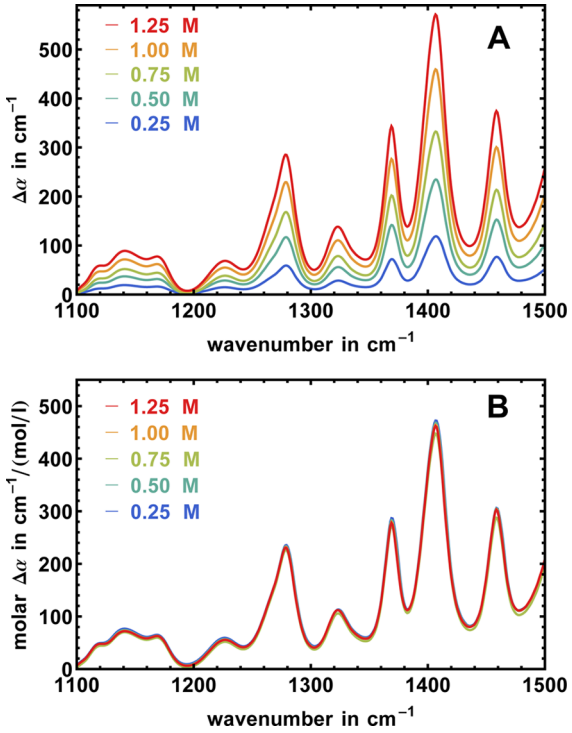

Figure 3. (A) Shown is the difference in absorption to water vs wavenumber in a section of the IR range (1100−1500 cm^{-1}) for five concentrations of dialanine solutions. (B) Shown is the molar difference in absorption to water vs wavenumber in a section of the IR range (1100−1500 cm^{-1}) for five concentrations of dialanine solutions.

dx.doi.org/10.1021/jp3021358 | J. Phys. Chem. B 2012, 116, 10020−10025

this analysis was to predict the resonant modes. We used a local character indicator (P) to characterize quantitatively the localization of a normal mode on the dialanine molecule (analogue to ref 20):

$$P_I = \sum_{j=1}^{N_D} |\vec{y}_{Ij}|^2 \tag{10}$$

where N_D is the number of dialanine atoms and y_{Ij} is the Cartesian component of eigenvector I on atom j. The partial contribution of the dialanine atoms gives the fraction of the (normalized) eigenvector due to the dialanine molecule. If the indicator value is one ($P_I = 1$), only the dialanine molecule is contributing to the motion; if the indicator decreases, more and more water molecules are involved. The modes were collected into bins of 1 cm^{-1}. The result of the simulation is plotted in Figure 4. As can be seen there, all modes, which are mainly

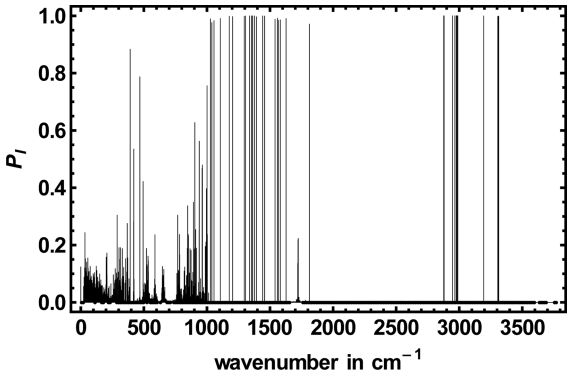

Figure 4. Displayed is P_I the local character indicator of the normal mode I in bins of 1 cm^{-1} vs the absorption (driving) frequency.

located on the dialanine ($P_I > 0.9$), are restricted to frequencies above 350 cm^{-1}. These can be attributed to localized intramolecular modes of dialanine. In the lower frequency range, the modes are found to be less localized: Within the investigated frequency range (0−250 cm^{-1}), none of these has a value of more than $P_I = 0.25$. These modes can be assigned to coupled dialanine−water motions.

In the IR frequency range, we find specific intramolecular resonances of the dialanine with $P_I \approx 1$. For a more specific investigation, we have selected a resonance at 1013 cm^{-1}. As was expected from the broad absorption band in the range between 20 and 90 cm^{-1}, it is not possible to identify such a localized solute mode in the THz range.

The resulting average absorbed energy when driving the dialanine between 20 and 90 cm^{-1} is shown in Figure 5. As can be seen, the maximum of this broad resonance is close to 81.9 cm^{-1}.

In Figure 6, the average absorbed energy of the mode at 81.9 cm^{-1} is plotted as a function of time. We have separated the average absorbed energy into two parts, which describe the contribution of dialanine and water, respectively. As the solute is driven, at the very beginning (within the first 0.5 ps), the average absorbed energy of the solute is increasing rapidly. However, after 0.5 ps, a plateau is reached and the energy remains nearly constant at about 1 kcal/mol. Thereafter, only small fluctuations due to the driving frequency can be observed. Starting at 0.25 ps, we find a continuous increase of the average absorbed energy in the solvent. Additionally, in Figure 6, we have partitioned the average absorbed energy of the water into

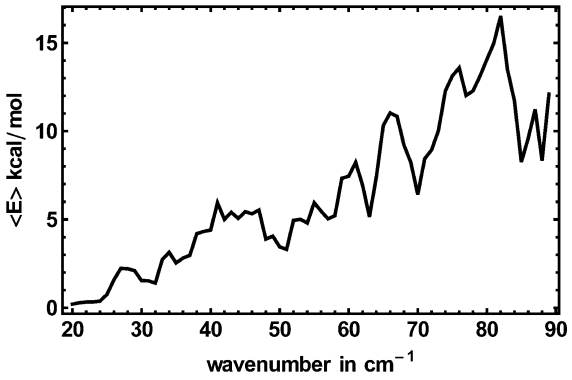

Figure 5. Average absorbed energy as a function of frequency from 20 to 90 cm^{-1} (frequency resolution 1 cm^{-1}) for a driving time of 10 ps with a coupling constant of 10^{-4} Hartree/bohr.

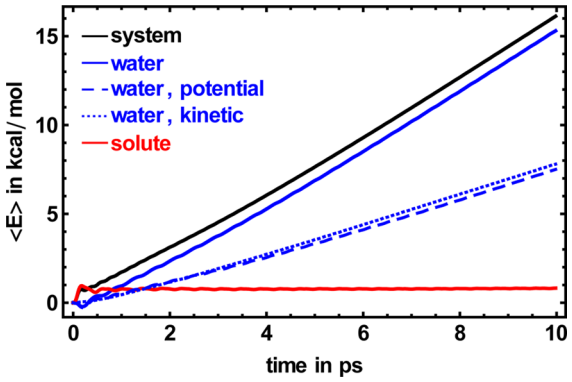

Figure 6. Average absorbed energy when driving at 81.9 cm^{-1} with a coupling constant of 10^{-4} Hartree/bohr. The blue dashed and dotted lines show the partitioning of the average absorbed energy of the water molecules into potential and kinetic energy, respectively.

two parts: the potential and kinetic energy. The initial decrease ($t < 0.5$ ps) in the potential energy is caused by movement of the dialanine. Afterward, both kinetic and potential energy increase constantly over 10 ps up to about 7.5 kcal/mol for the potential energy and about 8 kcal/mol for the kinetic energy.

In order to get more insights into the energy flow in the water, we performed a simulation with an even larger box, containing 3993 water molecules and the dialanine. Figure 7 displays the results for the average absorbed kinetic energy per water molecule when driving the resonance at 81.9 cm^{-1}: We

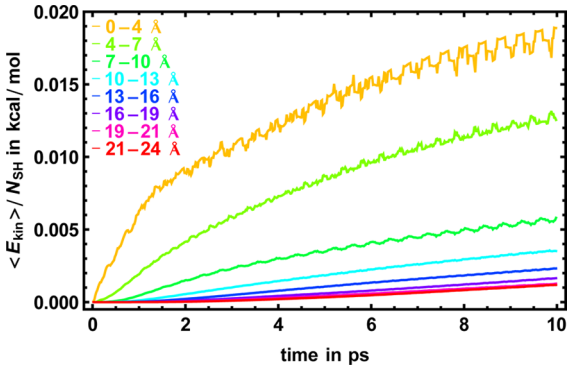

Figure 7. Average absorbed kinetic energy per water molecule when driving at 81.9 cm^{-1} with a coupling constant of 10^{-4} Hartree/bohr. The average absorbed energy is partitioned in shells around the solute.

dx.doi.org/10.1021/jp3021358 | J. Phys. Chem. B 2012, 116, 10020−10025

have partitioned the total absorbed energy in the absorbed energy of successive hydration shells, each of which is 3 Å thick (besides the first with a thickness of 4 Å). More in detail, we have considered water molecules within a distance of 0−4, 4−7, 7−10, 10−13, 13−16, 16−19, 19−21, 21−24, and 24−27 Å. The result is displayed in Figure 7: After an onset (e.g., 1 ps for the first shell), we find a continuous increase of energy, which is delayed the farther away each shell is displaced from the solute. The average absorbed kinetic energy of the first shell (0−4 Å) increases rapidly. In the initial picosecond, the increase is nearly linear; after about 2 ps, the slope decreases with time. This is correlated with a sharp rise of the kinetic energy for the subsequent shells. Additional small fluctuations are caused by water molecules, which leave or enter the boundary of a specific shell.

We find a different behavior in the IR. The results when driving an intramolecular mode of dialanine at 1012.7 cm^{-1} are shown in Figure 8. Here, the total average absorbed energy

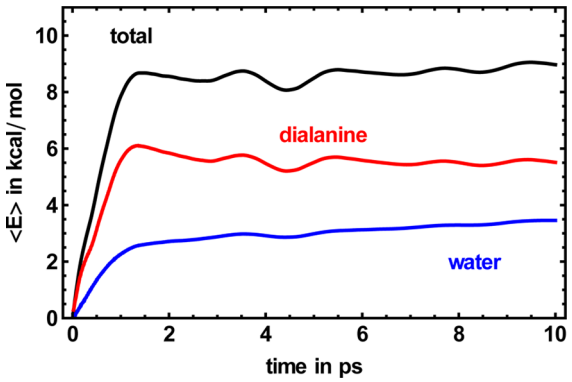

Figure 8. Average absorbed energy when driving at 1012.7 cm^{-1} with a coupling constant of 10^{-4} Hartree/bohr as a function of time.

increases within the first picosecond to about 8.5 kcal/mol. After this initial increase, we find a slower rise up to about 9 kcal/mol after 10 ps. Small fluctuations caused by the driving frequency can be seen. Whereas the average absorbed energy of the solute raises rapidly in the first ps up to about 6 kcal/mol, we find a slight decrease after this to about 5.5 kcal/mol. The average absorbed energy of the water increases rapidly within 1 ps to about 2.5 kcal/mol. Later, we find a less pronounced increase up to a maximum of 3.5 kcal/mol.

DISCUSSION AND CONCLUSION

In Figure 9, we have summarized our results for the storage of the kinetic energy in the THz and IR range, when driving the solute. For this, we have used a color-coding which shows the stored energy (given in units of K). In the THz range, we observe a very rapid flow of energy into the solvent which results in a heating of the solute and the surrounding water molecules. In contrast, when exciting at a mode in the IR, the energy is stored in the solute and the solvent remains cold. This is attributed to the efficient coupling of the high density of water modes with the solute excitation in the THz range. Using *ab initio* MD study, we have been able to characterize the low frequency modes of water more in detail.[21] This study allowed us to dissect the spectrum and assign the modes around 90 cm^{-1} to collective correlated particle motions extending over at least 7 Å. The results of the present study show a highly efficient flow of energy from the low frequency solute modes to

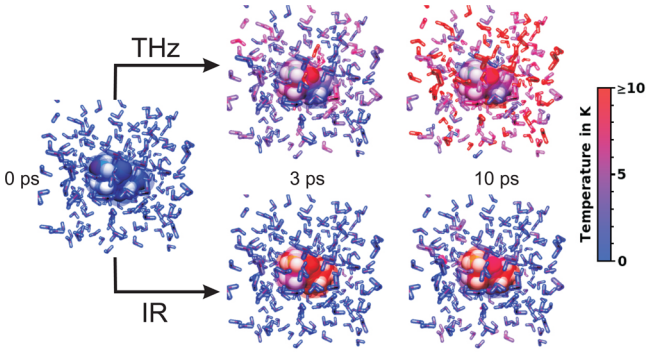

Figure 9. Illustration of the kinetic energy of the dialanine molecule and the 200 surrounding water molecules before driving and after driving for 3 and 10 ps, respectively, at the frequencies 81.9 cm^{-1} (THz) and 1012.7 cm^{-1} (IR).

those of the solvent. It has been shown in our previous study that this efficient coupling between the solute and solvent in the THz takes place via particle motions.

In summary, we find major differences for the flow of energy from the solute to the solvent exciting either in the IR or THz spectral range. Whereas a rapid energy flow to and across the water network is found in the THz range, in the IR we find that most of the energy is stored in localized modes of the peptide. The average absorbed energy when driving a mode at 1012.7 cm^{-1} results in a short rapid increase in energy, but after about one ps, we find only a small increase in the average absorbed energy. Only a small amount of energy is transferred from the dialanine to the water after the initial rise. In contrast, for the excitation of the THz mode at 81.9 cm^{-1}, we find that most of the energy is transferred in the water network, which results in a continuous energy flow from the solute to the solvent.

The efficient coupling requires the development of new concepts in the THz range. These concepts are expected to differ from those used for dielectric studies, which attribute the observed change exclusively to local changes in reorientational dynamics of water[22] as well as from those developed for IR spectroscopy (localized modes). Neither of these holds in the THz.

AUTHOR INFORMATION

Corresponding Author

*E-mail: Martina.Havenith@rub.de.

Notes

The authors declare no competing financial interest.

ACKNOWLEDGMENTS

The work of G.N. was supported by the Ruhr-University Research School funded by Germany's Excellence Initiative [DFG GSC 98/1] and the DAAD (German Academic Exchange Service).

REFERENCES

(1) Botan, V.; Backus, E. H. G.; Pfister, R.; Moretto, A.; Crisma, M.; Toniolo, C.; Nguyen, P. H.; Stock, G.; Hamm, P. *Proc. Natl. Acad. Sci. U.S.A.* **2007**, *104*, 12749−12754.

(2) Leitner, D. M. *Annu. Rev. Phys. Chem.* **2008**, *59*, 233−259.

(3) Kim, Y. S.; Wang, J.; Hochstrasser, R. M. *J. Phys. Chem. B* **2005**, *109*, 7511−7521.

(4) Agbo, J. K.; Leitner, D. M.; Myshakin, E. M.; Jordan, K. D. *J. Chem. Phys.* **2007**, *127*, 064315-1−064315-10.

(5) Rejto, P. A.; Bindewald, E.; Chandler, D. *Nature (London)* **1995**, *375*, 129−31.
(6) Fujisaki, H.; Zhang, Y.; Straub, J. E. *J. Chem. Phys.* **2006**, *124*, 144910−1−10.
(7) Zhang, Y.; Fujisaki, H.; Straub, J. E. *J. Phys. Chem. A* **2009**, *113*, 3051−3060.
(8) Bowman, J. M.; Zhang, X.; Brown, A. *J. Chem. Phys.* **2003**, *119*, 646−650.
(9) Kaledin, M.; Brown, A.; Kaledin, A. L.; Bowman, J. M. *J. Chem. Phys.* **2004**, *121*, 5646−5653.
(10) Kaledin, M.; Kaledin, A. L.; Bowman, J. M. *J. Phys. Chem. A* **2006**, *110*, 2933−2939.
(11) Kaledin, M.; Kaledin, A. L.; Bowman, J. M. Driven molecular dynamics for normal modes of biomolecules without the Hessian, and beyond. *Normal mode analysis: Theory and applications to biological and chemical systems*; CRC Press: 2006; pp 281−300.
(12) Niehues, G.; Heyden, M.; Schmidt, D. A.; Havenith, M. *Faraday Discuss.* **2011**, *150* (1), 193−207.
(13) Funkner, S.; Niehues, G.; Schmidt, D.; Heyden, M.; Schwaab, G.; Callahan, K.; Tobias, D. J.; Havenith, M. *J. Am. Chem. Soc.* **2012**, *134* (2), 1030−1035.
(14) *TINKER, Software Tools for Molecular Design*, version 4.1; Washington University School of Medicine, June 2003, available from http:// dasher.wustl.edu/tinker.
(15) Damm, W.; Frontera, A.; Tirado-Rives, J.; Jorgensen, W. L. *J. Comput. Chem.* **1997**, *18*, 1955−1970.
(16) Dang, L. X.; Pettitt, B. M. *J. Phys. Chem.* **1987**, *91*, 3349−3354.
(17) Nocedal, J.; Wright, S. J. *Numerical Optimization*; Springer: New York, 1999; pp 222−228.
(18) Leitner, D. M.; Gruebele, M.; Havenith, M. *HFSP J.* **2008**, *2* (6), 314−323.
(19) Dyke, S. H.; Hedwig, G. R.; Watson, I. D. *J. Solution Chem.* **1981**, *10*, 321−331.
(20) Brooks, B. R.; Janezic, D.; Karplus, M. *J. Comput. Chem.* **1995**, *16*, 1522−1542.
(21) Heyden, M.; Sun, J.; Funkner, S.; Mathias, G.; Forbert, H.; Havenith, M.; Marx, D. *Proc. Natl. Acad. Sci. U.S.A.* **2010**, *107* (27), 12068−12073.
(22) Tielrooij, K. J.; Garcia-Araez, N.; Bonn, M.; Bakker, H. J. *Science* **2010**, *328*, 1006−1009.